Effect of input data in the impact studies of road traffic noise in a time-domain model

Gwenaël GUILLAUME[1]; Benoit GAUVREAU[1]

[1] LUNAM Université, IFSTTAR, AME, LAE, Centre de Nantes, CS 4, Route de Bouaye, 44341 Bouguenais, France

ABSTRACT

The design of efficient screens for preventing noise exposure close to road lanes with high traffic flow is both a technical and an economical stake. This design (including material properties) is usually carried out upstream to *in-situ* realizations through numerical predictions. However, the uncertainties concerning the input data can lead to strong discrepancies in SPL predictions that are not considered in such impact studies. For instance, the modelling of the road traffic flow stands for a key point. Likewise, the surfaces properties (ground, screens materials, etc.) and the atmospheric conditions (inside and outside the urban canopy) can affect the sound propagation at relatively short distance when considering urban areas. Those scientific topics are currently under consideration in the framework of a french national project called EUREQUA. Thus, the present work treats about this project results by focussing on the effect of such input data in a time-domain model based on the transmission line matrix method.

Keywords: time-domain model, input data, coherent line source, incoherent line source
I-INCE Classification of Subjects Number(s): 76.1

1. INTRODUCTION

Dealing with environmental noise requires an appropriate modelling of road traffic noise, *i.e.* the simulation of line sources for far-field. As underlined in Ref. (1), the consideration of coherent line sources results in overestimating the insertion losses of noise barriers. Moreover, the use of a coherent line source instead of an incoherent line source causes strong destructive interferences (2) and tends to increase the dominance of the modes in a circulating street (3). Nevertheless, if considering sound pressure levels relative to free field, the coherent line source solution leads to equivalent results as a point source solution (4). Most of all, an incoherent line source stands for a better approximation of traffic noise sources since it corresponds to the sum of totally uncorrelated point sources, whereas a coherent line source corresponds to sources emitting in phase (1). Moreover, an incoherent line source of finite length stands for a more pragmatic depiction of a traffic flow (3, 5, 6).

For the modelling of far-field sound pressure levels, an incoherent line source can be modelled by considering a continuous sum of independent point sources. Thus, point sources which make up the line source emit one after the other a pulse signal. On the contrary, a coherent line source is implemented as an array of point sources which synchronously emits a pulse signal. The present study deals with the depiction of a line source by an array of point sources. The paper focusses on the effect of the spatial distribution of the point sources in order to create an incoherent line source while minimizing the standard deviation on the sound pressure levels according to the sources trigger. First, the modelling of coherent and incoherent line sources is presented. Then, the calculation configuration is detailed. Finally, results in terms of sound pressure levels spectra per third octave bands are given and discussed regarding dispersion according to the line source discretization.

2. COHERENT/INCOHERENT LINE SOURCE

A coherent line source stands for a set of point sources emitting in-phase signals. For time-domain approaches, a coherent line source is then modelled by introducing a finite number of sound sources with synchronous and identical emission (*i.e.* the same signal is produced by all point sources with matching time evolution). On the contrary, considering incoherent sources means that no relation of phase exists between point sources which compose the line source. In time-domain models, an incoherent line source is thus modelled

[1] gwenael.guillaume@ifsttar.fr

by assigning a random phase at each point source constituting the line source (6). Consequently, each point source emission is uncorrelated with others points sources emission.

However, the modelling of incoherent line sources by randomly trigger the sound sources requires to perform several simulations as some particular interferences occur between the propagated signals according to the trigger selection (6). Then, the distribution of the line source energy according to the line source discretization have to be assessed in order to limit the number of simulations, even to allow a good representativeness of an incoherent line source through a single calculation.

3. GEOMETRICAL AND NUMERICAL CONFIGURATIONS

3.1 Computational domain

Line source modelling is studied with the 3D computational domain depicted at Figure 1. The line source is placed along the y-axis upon a perfectly reflecting boundary in order to simulate a propagation medium where this boundary would be the axis of symmetry, *i.e.* a domain twice as much larger as the simulated domain. All sources S_i ($i = 1$ to n) are located at 0.3 m high above the ground and separated by a distance d varying according to the simulations (*see* Section 3.3). Two receivers R_1 and R_2 are located 1.5 m above ground, at 10 m and 20 m from the the center of the sources axis along the x-axis respectively. Apart from the line source boundary and the ground, the propagation medium is surrounded with absorbing layers (7).

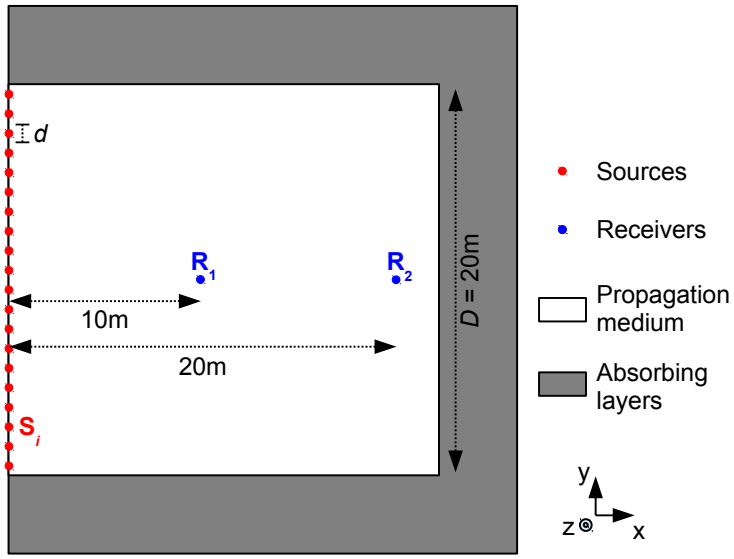

Figure 1 – Horizontal cut-off of the 3D propagation medium for the study of the line sources modelling. Sources and receivers are located at 0.3 m and at 1.5 m high above the ground respectively.

3.2 Line sources modelling

Line sources (coherent or incoherent) are simulated by regularly distributing N point sources along their axis. Considering n point sources S_i separated from each other a distance d (what is equivalent as considering line source segments of length d with a centered point source), each point source emitting a time signal $s_i(t)$ with a fixed amplitude A_i, *i.e.* an identical sound level L_i, the total emission sound level $L_{\Sigma,n}$ can be estimated by:

$$L_{\Sigma,n} = 10\log_{10}\left(n\,10^{L_i/10}\right) = 10\log_{10}\left(n\frac{|s_i|^2}{p_{\text{ref}}^2}\right), \tag{1}$$

with p_{ref} the reference sound pressure ($p_{\text{ref}} = 2\cdot 10^{-5}$ Pa).

For a coherent line source, each point source signal $s_{\text{coh}_i}(t)$ corresponds to a gaussian-shape time signal starting at $t = 0$ of the following form:

$$s_{\text{coh}_i}(t) = A_i \exp\left[\left(-\pi^2\left(f_{\text{src}}\,t - 1\right)^2\right)\right], \tag{2}$$

where f_{src} is the source frequency defined as $f_{\text{src}} = \frac{f_{\max}}{2}$ (with $f_{\max}$ the maximal frequency of validity of the simulation). In the case of an incoherent line source, the point source signals $s_{\text{incoh}_i}(t)$ are similar to the

coherent ones but their emission triggers are shifted with respect to each others by a time decay t_i particular to each point source S_i such as:

$$s_{\text{incoh}_i}(t) = A_i \exp\left[\left(-\pi^2 f_{\text{src}}(t-t_i)^2\right)\right]. \quad (3)$$

Each source sound power $L_{\text{W,i}}$ is defined in dB.m^{-1} which can be expressed as a function of the total sound level $L_{\Sigma,n}$:

$$L_{\Sigma,n} = D \cdot L_{\text{W},i} = n \cdot d \cdot L_{\text{W},i}, \quad (4)$$

with D the length of the line source. Thus, each signal amplitude can be estimated as a function of the sound power per meter $L_{\text{W,m}}$ and of the number of point sources per meter $N_{\text{src/m}} = 1/d$, that is combining Eqs. (1) and (4):

$$A_i = \frac{p_{\text{ref}}}{\sqrt{n}} 10^{nL_{\text{W,m}}/20N_{\text{src/m}}}. \quad (5)$$

The same formula is used for a coherent (Eq. (2)) and a incoherent (Eq. (3)) line source .

In order to uncorrelate the signals of point sources (*i.e.* to simulate an incoherent line source), the time decay t_i of each point source is randomly selected for each segment. Thus, the time required to ensure the emission by the whole point sources and the propagation up to the receivers increases by refining the discretization of the line source (*see* Table 1). In the case of the coherent line sources, the simulation duration remains identical in either line source discretization cases and fixed at 0.107 s for this geometrical and numerical configuration (Figure 1). The time decay between each point source trigger is equal to the gaussian pulse duration (*i.e.* 0.013 s). Thus, the effect of the time decay is not considered in the present study.

3.3 Simulations parameters

Calculations are performed with the Transmission Line Matrix (TLM) model (8, 9, 10). The computational domain presented at Figure 1 is discretized with a spatial step equal to 0.05 m which implies a validity for the calculations until the nominal frequency at 650 Hz for third octave band analysis. The associated time discretization is around $8.5 \cdot 10^{-5}$ s. The ground is assumed as perfectly rigid and the propagation conditions are homogeneous (no wind or temperature effects). The absorbing layers are designed such as allowing a frequency domain analysis from the 100 Hz nominal frequency.

The calculations consist in simulating alternatively a coherent or an incoherent line source with various line source discretizations d (*see* Figure 1). In each case of incoherent line source with a constant discretization, 5 simulations are performed with different sources trigger. In order to reduce the duration of the emission, the line source is divided into point sources arrays of 10 m long (*i.e.* 2 arrays for this geometry). Thus, 5 different selections of sources triggers can be simulated for the larger discretization step evaluated in this study (*i.e.* $d = 2$ m, *see* Table 1). Such calculations are repeated by varying the discretization of the line source from $d = 0.05$ m until $d = 2$ m and adapting the signals amplitude according to the number of point sources per meter $N_{\text{srcs/m}}$ in order to approximate a line source with a sound energy $L_{\text{W,m}} = 90$ dB.m^{-1}. In total, 5 line source discretizations are considered which are reported in Table 1 with their associated number of sources in total n and per meter $N_{\text{srcs/m}}$, as well as their associated number of sources per both minimal and maximal wavelengths ($N_{\text{srcs/}\lambda_{\text{min}}}$ and $N_{\text{srcs/}\lambda_{\text{max}}}$ respectively), and the simulated time of propagation.

Table 1 – Simulated line source discretizations and associated number of sources in total n and per meter $N_{\text{srcs/m}}$, as well as per both minimal $N_{\text{srcs/}\lambda_{\text{min}}}$ and maximal $N_{\text{srcs/}\lambda_{\text{max}}}$ wavelengths ($\lambda_{\text{min}} = 3.4$ m and $\lambda_{\text{max}} = 0.52$ m), and the simulated time of propagation.

d (m)	n	$N_{\text{srcs/m}}$	$N_{\text{srcs/}\lambda_{\text{min}}}$	$N_{\text{srcs/}\lambda_{\text{max}}}$	Simulated time (s)
0.10	200	10	34.0	5.2	1.50
0.25	80	4	13.6	2.1	0.63
0.50	40	2	6.8	1.0	0.37
1.00	20	1	3.4	0.5	0.24
2.00	10	0.5	1.7	0.3	0.18

4. RESULTS AND DISCUSSION

Figure 2 shows the sound pressure level per third octave bands nominal frequency at microphones R_1 and R_2 (at 10 m and 20 m from the central point source respectively) as a function of the number of sources per meter

$N_{\text{srcs/m}}$ used for modelling both the coherent and incoherent line sources. Unsurprisingly, the decrease of the sound levels deviations when refining the incoherent line source discretization (blue error bars) appears mainly at low frequencies for both receivers. Nevertheless, the calculation of the source signals amplitude according to the number of point sources (Eq. (5)) does not give expected results, especially for $N_{\text{srcs/m}} = 2$ sources per meter whatever the frequency, what is surely linked to the microphones geometry. For both microphones, the coherent line source (in red) mainly leads to higher sound pressure levels than the incoherent one (in blue).

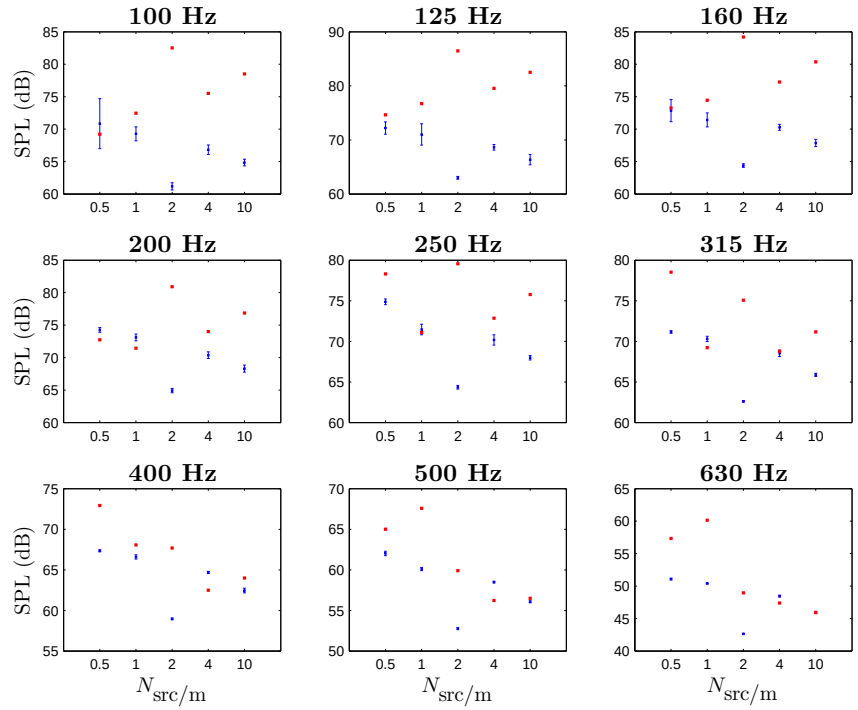

(a) R_1

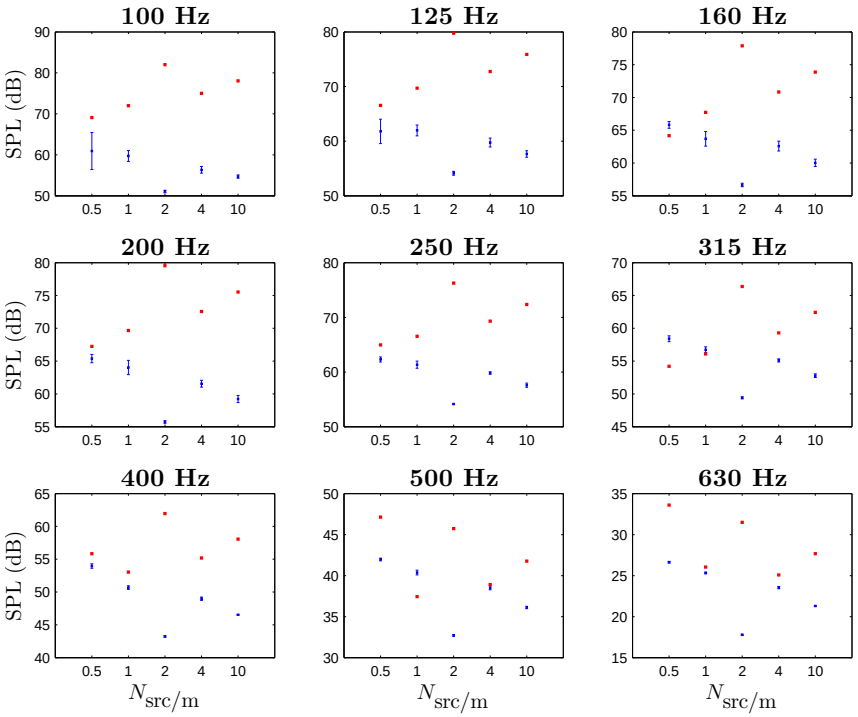

(b) R_2

Figure 2 – Sound pressure level spectra per third octave bands at microphones (a) R_1 and (b) R_2 according to the number of sources per meter $N_{\text{srcs/m}}$ of the line source for both coherent (in red) and incoherent (in blue) line sources. The error bars represent two times the standard deviation.

In order to free from the sources amplitude deviation according to the incoherent line source discretization, another representation is proposed at Figure 3 which displays the sound pressure level spectra per third octave bands at microphone R_2 relative to microphone R_1 as a function of the number of sources per meter $N_{srcs/m}$, for the incoherent line source solely. The mean spectra (in blue at Figure 3a and linearly interpolated between both the numbers of sources per meter $N_{srcs/m}$ and nominal frequencies at Figure 3b) is similar regardless the line source discretization except at low frequencies (*i.e.* below 315 Hz) for $N_{srcs/m} < 2$, *i.e.* from a number of point sources per maximal wavelength $N_{srcs/\lambda_{max}} = 1$ (*see* Table 1).

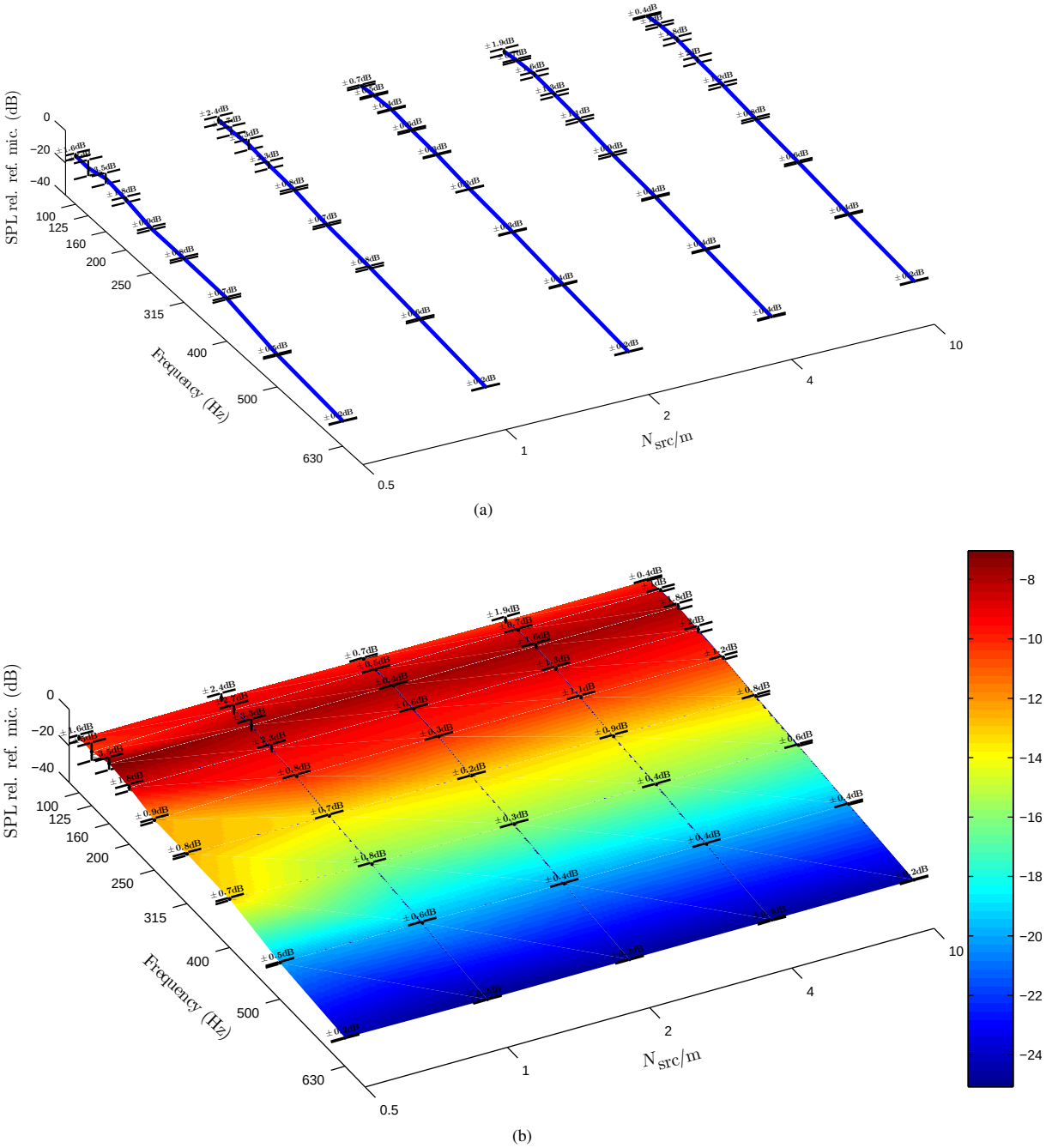

Figure 3 – Sound pressure level spectra per third octave bands at microphone R_2 relative to microphone R_1 according to the number of sources per meter $N_{srcs/m}$ of the incoherent line sources: (a) mean spectra (in blue) and (b) mean sound pressure levels interpolated between both the nominal frequencies and numbers of sources per meter $N_{srcs/m}$. The error bars represent two times the standard deviation.

The dispersion at each nominal frequency is more easily analysable from Figure 4 which shows the standard deviation of the sound pressure level spectra per third octave bands at microphone R_2 relative to microphone R_1 according to the number of sources per meter $N_{srcs/m}$. Similarly to Figure 3b, the sound pressure levels

are linearly interpolated between both the nominal frequencies and numbers of sources per meter $N_{\text{srcs/m}}$. The largest deviations appear only at low frequency for all line sources discretizations, in particular for $N_{\text{srcs/m}} < 2$. According to these results for this geometry (Figure 1), it seems more appropriate to model an incoherent line source by using a discretization over 2 sources per meter in order to minimize the standard deviation of the sound pressure levels related to the trigger order of uncorrelated sources.

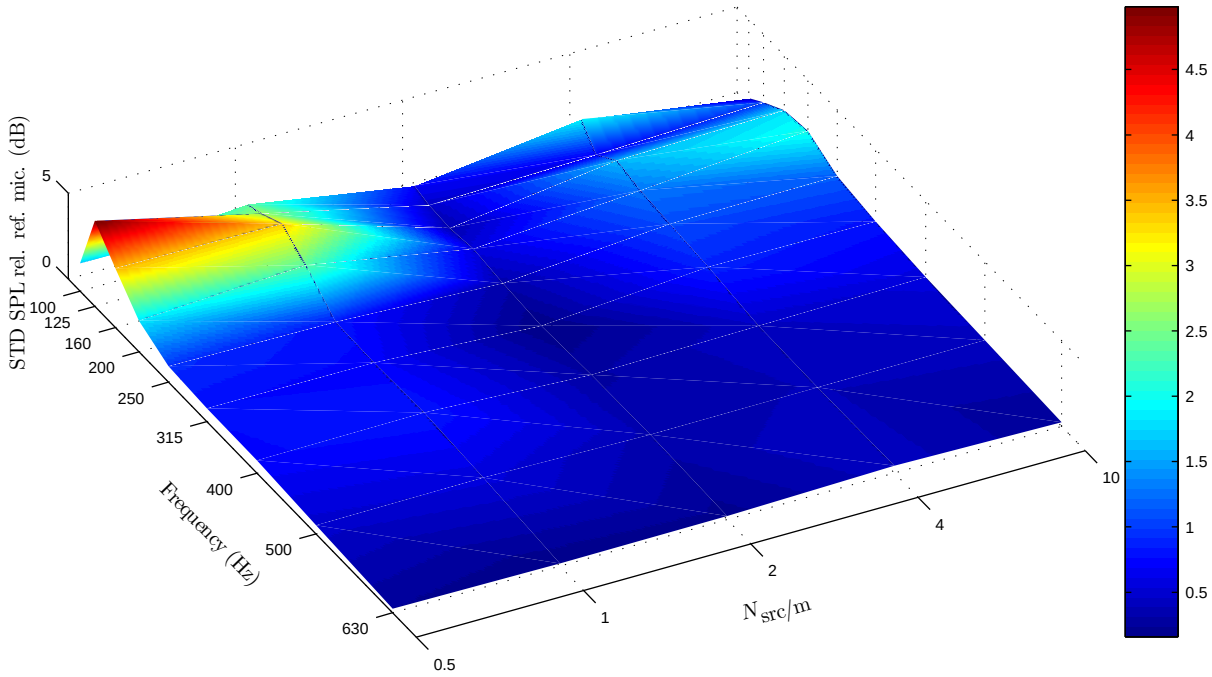

Figure 4 – Standard deviation of the sound pressure level spectra per third octave bands at microphone R_2 relative to microphone R_1 according to the number of sources per meter $N_{\text{srcs/m}}$ of the incoherent line sources. The sound pressure levels are linearly interpolated between both the numbers of sources per meter $N_{\text{srcs/m}}$ and nominal frequencies.

5. CONCLUSION

The modelling of a road traffic lane stands for a key point for environmental acoustics applications. An incoherent line source is more appropriate when simulating such sources at far-field. The present paper deals with the modelling of line sources in a time-domain model by studying the effect of the discretization of the line source into an array of point sources. Results show that an incoherent line source implies less sound pressure levels dispersion if distributing the sound energy over at less 2 point sources per meter for the considered geometry. Future works will consists in improving the management of the amplitude of point sources signals according to the discretization of the line source and in introducing traffic flow parameters as the number of vehicles per hour and the traffic velocity (11, 12). Others input data influences should also be assessed in the future, such as the source height above ground, the ground properties (*e.g.* the impedance characteristics), the meteorological conditions, etc.

ACKNOWLEDGEMENTS

This research lies within the framework of the projet ANR-11VILD-0006 named Eurequa, financially supported by the French National Reseaarch Agency (ANR).

REFERENCES

1. Jean P, Defrance J, Gabillet Y. The importance of source type on the assessment of noise barriers. Journal of Sound and Vibration. 1999;226(2):201–216. Available from: `http://www.sciencedirect.com/science/article/pii/S0022460X99922733`.

2. Van Renterghem T, Bottledooren D. Numerical evaluation of sound propagating over green roofs. Journal of Sound and Vibration. 2008 November;317(3-5):781–799.

3. Hornikx M, Forssén J. Noise abatement schemes for shielded canyons. Applied Acoustics. 2009 February;70(2):267–283.

4. Van Renterghem T, Salomons EM, Botteldooren D. Efficient FDTD-PE model for sound propagation in situations with complex obstacles and wind profiles. Acta Acustica united with Acustica. 2005 August;91(4):671–679.

5. Duhamel D. Efficient calculation of the three-dimensional sound pressure field around a noise barrier. Journal of Sound and Vibration. 1996;197(5):547–571.

6. Van Renterghem T, Botteldooren D, Verheyen K. Road traffic noise shielding by vegetation belts of limited depth. Journal of Sound and Vibration. 2012;331(10):2404–2425.

7. Guillaume G, Picaut J. A simple absorbing layer implementation for transmission line matrix modeling. Journal of Sound and Vibration. 2013;332(19):4560–4571.

8. Guillaume G, Picaut J, Dutilleux G, Gauvreau B. Time-domain impedance formulation for transmission line matrix modelling of outdoor sound propagation. Journal of Sound and Vibration. 2011;330(26):6467–6481.

9. Guillaume G, Aumond P, Gauvreau B, Dutilleux G. Application of the transmission line matrix method for outdoor sound propagation modelling – Part 1: Model presentation and evaluation. Applied Acoustics. 2014;76:113–118.

10. Aumond P, Guillaume G, Gauvreau B, Lac C, Masson V, Bérengier M. Application of the Transmission Line Matrix method for outdoor sound propagation modelling – Part 2: Experimental validation using meteorological data derived from the meso-scale model Meso-NH. Applied Acoustics. 2014;76:107–112.

11. Jonasson HG. Acoustical Source Modelling of Road Vehicles. Acta Acustica United with Acustica. 2007;93:173–184.

12. Hornikx M, Forseén J. Modelling of sound propagation to three-dimensional urban courtyards using the extended fourier PSTD method. Applied Acoustics. 2011;72:665–676.